

# Some new results for “jet” stopping in AdS/CFT (long version)<sup>‡</sup>

Peter Arnold and Diana Vaman

Department of Physics, University of Virginia, Box 400714, Charlottesville,  
Virginia 22904, USA

E-mail: [parnold@virginia.edu](mailto:parnold@virginia.edu), [dv3h@virginia.edu](mailto:dv3h@virginia.edu)

**Abstract.** We give a breezy, qualitative overview of some of our recent results [1, 2] on studying jet stopping in strongly-coupled plasmas using gauge-gravity duality. Previously, people have found that the maximum stopping distance in such plasmas scales with energy as  $E^{1/3}$ . We show that there is an important distinction between typical and maximum stopping distances. For the strongly-coupled excitations that we study, we find that the typical stopping distance scales with energy as  $E^{1/4}$ .

How far does a high-energy excitation travel through a quark-gluon plasma, before it stops in the medium and thermalizes? To get the discussion started, consider the weak-coupling picture of energy loss depicted in fig. 1, which is dominated by nearly-collinear bremsstrahlung at high energy. What sets the scale for the running coupling constant in this process? As the particle flies along, it picks up small kicks from the medium, which change its direction, which is a form of acceleration, and so a source for bremsstrahlung. The individual kicks are dominated by relatively soft momentum scales for which  $\alpha_s$  is of order  $\alpha_s(T)$  (shown in red). But now consider the  $\alpha_s$  (shown in blue) associated with the emission of the bremsstrahlung gluon. Its scale is plausibly set by the relative transverse momenta  $Q_\perp$  of the two daughter particles after the splitting.<sup>§</sup> In an infinite medium (the relevant case if the medium is thick enough for a jet to actually stop), the typical  $Q_\perp$  grows slowly with particle energy as  $Q_\perp \sim (\hat{q}E)^{1/4}$ .<sup>||</sup> The scaling of the stopping distance  $l_{\text{stop}}$  depends on the size of  $\alpha_s$  at these two scales  $T$  and  $Q_\perp$ .

- *weak coupling:* If  $\alpha_s(T) \sim \alpha_s(Q_\perp)$  are both small, then  $l_{\text{stop}} \propto E^{1/2}$  (up to logarithms). This scaling is a corollary of the early work of Baier et al. (BDMPS) [4] and Zakharov [5] on the LPM effect in QCD. (For specific formulas for the stopping distance in weakly-coupled QCD, see ref. [6].)
- *mixed coupling:* If  $\alpha_s(T)$  is large and  $\alpha_s(Q_\perp)$  is small, various people have argued that the stopping distance still scales as  $l_{\text{stop}} \propto E^{1/2}$  and that the strong-coupling dynamics of the problem can be isolated into the value of  $\hat{q}$ . This is related, for

<sup>‡</sup> Talk given at Quark Matter 2011, Annecy, France, May 23–30, 2011. This is a long version of the 4-page paper submitted for publication in the conference proceedings.

<sup>§</sup> More specifically,  $Q_\perp$  is the typical transverse momentum picked up during the formation time of the bremsstrahlung gluon.

<sup>||</sup> See, for example, eq. (4.4b) of ref. [3], here parametrically extrapolated to the case  $\omega \sim E$ . This relation follows from the usual LPM relations that (for the case  $\omega \sim E$  of interest)  $t_{\text{form}} \sim E/Q_\perp^2$  and (for an infinite medium)  $Q_\perp^2 \sim \hat{q}t_{\text{form}}$ , where  $t_{\text{form}}$  is the formation time.

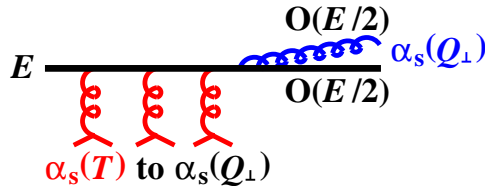


**Figure 1.** Weak-coupling picture of energy loss due to bremsstrahlung.

example, to the motivation of Liu, Rajagopal, and Wiedemann [7] to find the value of  $\hat{q}$  in strongly-coupled theories via AdS/CFT.

- *all strong coupling:* For  $\alpha_s(T) = \alpha_s(Q_\perp)$  very large, ¶ progress has been made in theories such as  $\mathcal{N}=4$  super Yang Mills (and its close cousins), where calculations are possible using gauge-gravity duality. In this case, people have found that the stopping distance has a different scaling with energy:  $l_{\text{stop}} \propto E^{1/3}$  [8, 9, 10].

In this article, we will focus on the last, all strong-coupling case. What is interesting about this result is its demonstration that the exponent  $\nu$  in  $l_{\text{stop}} \propto E^\nu$  can depend on  $\alpha_s$ . We will see that the strong-coupling case has an even richer set of exponents than  $l_{\text{stop}} \propto E^{1/3}$  to describe jet stopping.

Think about the finite-temperature 3+1 dimensional field theory, and imagine what happens if you very energetically kick the medium is some way at  $t=0$ , creating a localized excitation that moves through the medium, as depicted in fig. 2. At later times, one looks at the progress of the excitation through the medium by following some conserved density such as energy or momentum or charge density. For the purpose of this figure, it will be simplest if we think of charge density. As time passes, the charge density moves in a pulse that eventually slows down (because of energy loss) and then stops as the energy in the excitation thermalizes, after which the charge diffuses outward. The distance from the kick to the center of the late-time diffusion cloud of charge is the stopping distance.

As an example of previous calculations of jet stopping in AdS/CFT which found  $l_{\text{stop}} \propto E^{1/3}$ , we briefly review in fig. 3 how Chesler, Jensen, Karch, and Yaffe [10] set up the problem for light-quark jets. A classical string in the 5-dimensional gravity theory is used to describe a state analogous to a  $q\bar{q}$  pair in QCD. The string is initialized in a way that its end points fly apart, analogous to a high-energy back-to-back quark and anti-quark. As the ends fly apart, the string also falls in the fifth dimension towards the black brane horizon, as depicted by the time-series of curves, from top to bottom, in fig. 3a. The presence of the string disturbs the background gravitational and other fields, and so causes a deformation of the fields on the boundary, as depicted in fig. 3b. As in fig. 2, it will be pictorially simplest to discuss observing conserved charge densities which diffuse (rather than energy or momentum density, which can create sound waves). In the case of Chesler et. al, the relevant global charge is “baryon” number. As the string falls toward the horizon, its effect on the boundary becomes more and more red-shifted, and so spreads out to longer and longer wavelengths. This is how the falling string produces diffusion of the charge density seen in the boundary theory.

There is one just slightly dissatisfying aspect of this very nice picture: The initial

¶ More precisely  $N_c \alpha_s(T) = N_c \alpha_s(Q_\perp)$  very large for large- $N_c$   $\mathcal{N}=4$  super Yang Mills.

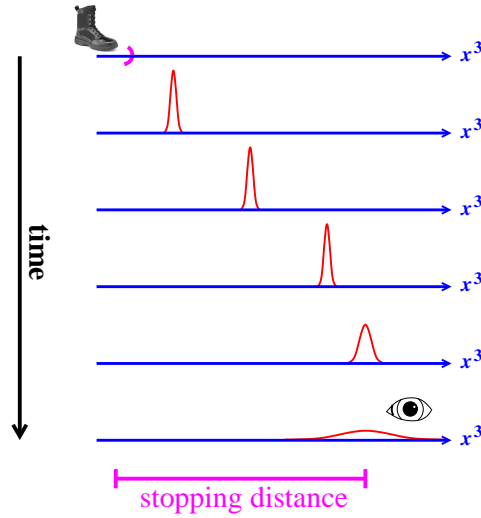


**Figure 2.** Evolution in time of a local excitation of some conserved charge created by a high-energy kick to the plasma. Here  $x^3$  means the third spatial coordinate, and the eyeball represents a late-time observation of the system.

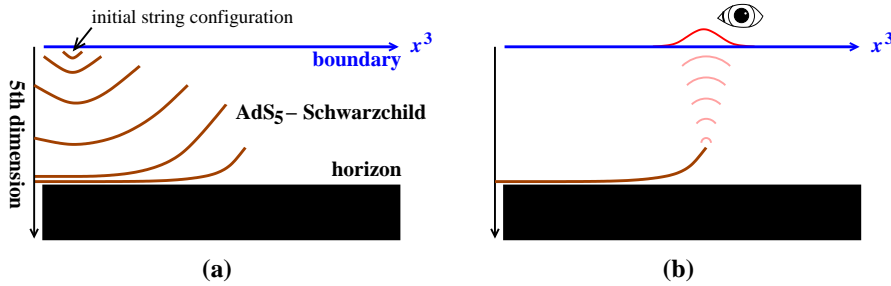


**Figure 3.** A cartoon of (a) the falling string of Chesler et. al [10] and (b) its effect on baryon number charge density on the boundary. See ref. [10] for their own versions of these cartoons.

configuration of the system has been specified in the language of the gravity dual rather than directly in the 3+1 dimensional field theory. Our goal is to avoid this by finding a way to formulate some “jet” stopping problem from beginning to end in the field theory. We will only use the gravity dual as a means to solve that field-theory problem.

To understand our method, it helps to first think impressionistically of the decay of a very high energy, slightly virtual photon, or of a very high energy  $W^+$  boson, in a QCD quark-gluon plasma. Fig. 4 shows the corresponding processes for weak coupling. Each creates a localized, high-energy, high-momentum excitation in the plasma, moving towards the right of the figure (the  $x^3$  direction). We will loosely call such an excitation a “jet.” In weakly-coupled QCD, the jet produced in fig. 4 starts out as a nearly-collinear  $q\bar{q}$  pair. In strongly-coupled  $\mathcal{N}=4$  SYM, the analogy is a

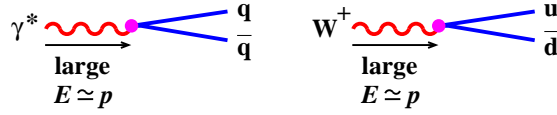


**Figure 4.** The decay of a high-energy slightly-virtual photon, or of a high-energy  $W^+$ , in a QCD quark-gluon plasma.

$$|\text{jet}\rangle = \text{boot} |\text{plasma}\rangle \quad (\text{a})$$

$$\langle \text{jet} | \text{eyeball} | \text{jet} \rangle = \langle \text{boot}^\dagger \text{eyeball} \text{boot} \rangle \quad (\text{b})$$

**Figure 5.** Schematic picture of how the expectation of an observable (eyeball) in a jet state created by some operator (boot) can be related to a 3-point equilibrium correlator.

localized excitation of strongly interacting gluons, gluinos, and adjoint scalars.

Now treat the red photon or  $W$  line in fig. 4 as an external field in the form of a high-energy plane wave  $e^{i\bar{k}\cdot x}$  with  $k^\mu = (E, 0, 0, E)$ . However, we will also approximately localize that external field, so that we know where the jet it creates starts from. That way, when we later see where the jet stops and thermalizes, we will be able to extract the stopping distance from the difference. Put all together, we replace the photon or  $W$  by adding a source term to the Lagrangian:

$$\mathcal{L}_{\text{QFT}} \rightarrow \mathcal{L}_{\text{QFT}} + \mathcal{O}(x) \Lambda_L(x) e^{i\bar{k}\cdot x} \quad (1)$$

with

$$\bar{k}^\mu = (E, 0, 0, E). \quad (2)$$

The factor  $\Lambda_L(x) e^{i\bar{k}\cdot x}$  is the external field, where  $\Lambda_L(x)$  is a smooth envelope function which localizes the source to a region of size  $L$  around the origin in both space and time. The  $\mathcal{O}(x)$  is the field-theory operator the external field couples to, such as  $j_\mu(x)$  in the examples of fig. 4, and corresponds to the vertex in fig. 4.

It turns out that the response to such a source is measured by a *3-point correlator* in the field theory. A crude but simple way to understand this is given in fig. 5. The boot represents the source operator in (1). We apply this operator to a generic state of the thermal plasma to create our localized, high-energy “jet” state, as in fig. 5a. We then want the expectation value in this state of some conserved density—energy or momentum or charge—represented by the eyeball operator in fig. 5b. Substituting fig. 5a into the left-hand side of fig. 5b yields the right-hand side of fig. 5b, which is a 3-point correlator of the boot, the eyeball, and the boot-conjugate, calculated for an equilibrium plasma.<sup>+</sup> For *finite-temperature* AdS/CFT calculations, there is a great deal in the literature on computing 2-point correlators, but until recently almost nothing carried through to specific results for 3-point correlators.

<sup>+</sup> The picture presented here is intended only for the sake of giving the reader a flavor for why 3-point correlators are involved. A better argument, in terms of response theory, is given in Sec. II.B of ref. [2]. The motivation given here, however, is somewhat akin to that of the zero-temperature work of Hofman and Maldacena [11]. See Sec. I.C of ref. [2] for a discussion of similarities and differences.

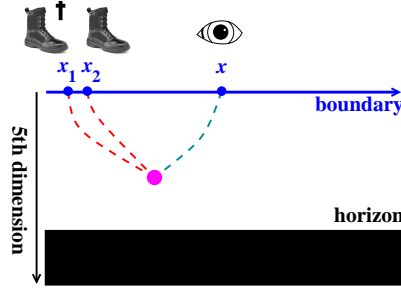


**Figure 6.** 3-leaf tree diagram that gives the 3-point correlator in the gravity dual theory.

To compute this field-theory three-point correlator, we use gauge-gravity duality to relate it to a three-point boundary correlator in  $\text{AdS}_5$ -Schwarzschild space, as depicted in fig. 6. Here  $x$  is the space-time point where we make our observation, and  $x_1$  and  $x_2$  are integrated over the source region. Recall that gauge-gravity duality relates the strongly-coupled field theory problem to a problem in *classical* gravity, which means tree diagrams in the gravity problem. In Fig. 6, we therefore have a three-leaf tree diagram made up of the dashed lines meeting at a vertex in the bulk. The vertex represents a cubic term in the 5-dimensional supergravity action. The dashed lines are bulk-to-boundary propagators and in our calculation are given by *Heun* functions. Heun functions are obscure generalizations of hypergeometric functions which are difficult to work with. As a result, it is difficult to make analytic progress in calculating generic 3-point functions, which requires integrating over the vertex position. It is also difficult to evaluate such integrals numerically in our problem because the fact that our source is high energy, and the fact that we are looking at real-time correlations, means that the bulk-to-boundary propagators associated with the boots are very highly oscillatory functions and so very difficult to integrate.

Fortunately, this very problem also points the way to a solution. The (red) dashed lines in fig. 6 associated with the boots are high-energy/momentum propagators, and we may make a corresponding high- $k$  WKB-like approximation, which gives them a relatively simple analytic form. For the remaining (green) dashed line in fig. 6, recall that the technique for measuring the stopping distance is to look for the spatial center of late-time charge diffusion, as depicted by the last curve in Fig. 2. This corresponds to measurements of large wavelengths and so small wave numbers of the late-time response of the system. As a result, we may use a low- $k$  approximation to the (green) dashed line associated with the eyeball in Fig. 6. The low- $k$  limit also gives a relatively simple analytic expression for the propagator. These approximations, appropriate for the problem we want to solve, turn out to be enough to make it possible to analytically integrate over the bulk vertex position and compute the 3-point correlator. [By the way, it is easy to see now why this physics could not possibly be captured by a 2-point correlator. If we took a 2-point correlator of a boot (source) and an eyeball (measurement), there would be a mismatch between the high-momentum of the boot and the low wave-numbers of interest for the eyeball, and so the 2-point correlator would vanish by momentum conservation.]

The results [1, 2] of using this method to calculate the jet stopping distance are summarized in Fig. 7, which shows a probability distribution for the jet stopping

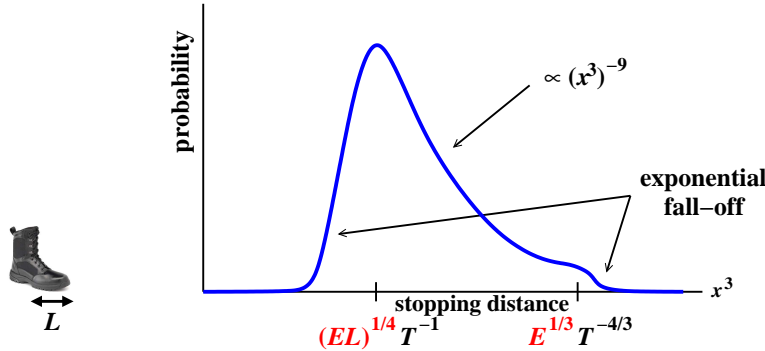


**Figure 7.** Qualitative picture of the probability distribution of jet stopping distances, where  $L$  is the source size. The power-law fall-off  $(x^3)^{-9}$  shown for the intermediate region is for the specific source operator analyzed in ref. [1]; the more general case is given in ref. [2].

distance. There is indeed a “maximum” stopping distance that scales like  $E^{1/3}$ , beyond which the probability distribution falls off exponentially. However, this is not the *typical* stopping distance of the jets created. Almost all of the jets created by our kick (1) instead stop sooner at a distance scale proportional to  $(EL)^{1/4}$ , where  $L$  is the size of the space-time region in which the jet was initially created (i.e. the size of the toe of our boot and the duration of the kick).<sup>\*</sup> Between the scales  $(EL)^{1/4}$  and  $E^{1/3}$ , the probability distribution falls algebraically, with the power law depending on the conformal dimension of the source operator [2].

By the way, for the  $x^3 \ll E^{1/3}T^{-4/3}$  case, which dominates the probability distribution shown in fig. 7, the calculation can be made even simpler than the forgoing discussion. In this limit, it turns out that one can use the approximation of geometric optics and replace the 3-point calculation of fig. 6 by a simple classical calculation of a 5-dimensional particle falling toward the horizon in AdS<sub>5</sub>-Schwarzschild space. See ref. [2] for details.

Readers may wonder what the size  $L$  of the source has to do with how far jets propagate? The answer is that  $L$  determines the virtuality of the source. Recall that in (1) we chose a source proportional to  $\Lambda_L(x) e^{i\vec{k}\cdot x}$  with  $\vec{k}^\mu = (E, 0, 0, E)$ . The envelope function  $\Lambda_L(x)$  localized the source to a region of size  $L$  and so, by the uncertainty principle, introduces a spread in momentum of size  $1/L$ . Fig. 8 gives a qualitative picture of the region of momentum space that contributes to  $\Lambda_L(x) e^{i\vec{k}\cdot x}$ . Generic momenta in this region are not exactly on the light cone, and we demonstrate in ref. [2] that the  $(EL)^{1/4}$  scaling of the typical stopping distance really means  $(E^2/q^2)^{1/4}$ , where  $q^2$  is the typical virtuality of the source:

$$l_{\text{typical}} \sim \left(\frac{E^2}{q^2}\right)^{1/4} \frac{1}{T}. \quad (3)$$

Studying jet stopping in the strongly-coupled limit is a useful theoretical exercise in order to sharpen our understanding of the role that coupling  $\alpha_s$  plays in the scaling

<sup>\*</sup> In the subject of jet quenching, the letter  $L$  is often instead used to stand for the thickness of the medium. This has nothing to do with our  $L$  here: in our problem, we are considering jet stopping in an infinite medium.

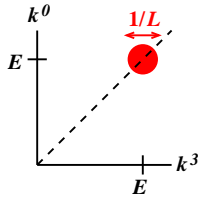


**Figure 8.** Qualitative picture of the region in 4-momentum where the source (1) has support.

of jet stopping with energy. It also provides an interesting test case for optimists, or a straw man for cynics, for phenomenological comparisons with data: Regardless of one’s point of view, AdS/CFT results inspire the question of whether experiment can differentiate between  $E^{1/2}$  and  $E^{1/3}$  or other scaling for jet stopping distances, or between non-standard scaling laws for other measurements related to energy loss. For some work along these lines, see refs. [12, 13, 14]. Readers who toy with such questions might naturally ask what happens if we now put  $q^2 \sim E^2$  into (3), since  $q^2 \sim E^2$  is the virtuality scale of processes creating high-energy jets at mid-rapidity in actual relativistic heavy ion collisions. The corresponding running coupling constant associated with the initial moments of such jet creation is  $\alpha_s(E)$ , rather than the couplings  $\alpha_s(T)$  or  $\alpha_s(Q_\perp)$  reviewed in the introduction. Whatever one may think of the theoretical or perhaps phenomenological utility of investigating jet stopping in strongly-coupled theories, it seems implausible that  $N_c \alpha_s(E)$  can be approximated as infinite for high energy jets. If there is any phenomenological application for the results presented here, one should likely avoid treating the system as strongly coupled until enough time has passed that the initial virtuality  $q^2 \sim E^2$  associated with jet creation has dropped to some lower virtuality where one is willing to at least entertain the possibility that the  $\alpha_s$  associated with the emission of a bremsstrahlung gluon might be effectively strongly coupled.

## Acknowledgments

This work was supported, in part, by the U.S. Department of Energy under Grant No. DE-FG02-97ER41027 and by a Jeffress research grant, GF12334.

## References

- [1] P. Arnold, D. Vaman, “Jet quenching in hot strongly coupled gauge theories revisited: 3-point correlators with gauge-gravity duality,” JHEP **10**, 099 (2010) [arXiv:1008.4023].
- [2] P. Arnold, D. Vaman, “Jet quenching in hot strongly coupled gauge theories simplified,” JHEP **04**, 027 (2011) [arXiv:1101.2689].
- [3] R. Baier, Y. L. Dokshitzer, A. H. Mueller, D. Schiff, “Quenching of hadron spectra in media,” JHEP **0109**, 033 (2001) [hep-ph/0106347].
- [4] R. Baier, Y. L. Dokshitzer, A. H. Mueller, S. Peigné and D. Schiff, “The Landau-Pomeranchuk-Migdal effect in QED,” Nucl. Phys. B **478**, 577 (1996) [arXiv:hep-ph/9604327]; “Radiative energy loss of high energy quarks and gluons in a finite-volume quark-gluon plasma,” Nucl. Phys. B **483**, 291 (1997) [arXiv:hep-ph/9607355]; “Radiative energy loss and  $p_\perp$ -broadening of high energy partons in nuclei,” Nucl. Phys. B **484**, 265 (1997) [arXiv:hep-ph/9608322].
- [5] B. G. Zakharov, “Fully quantum treatment of the Landau-Pomeranchuk-Migdal effect in QED and QCD,” JETP Lett. **63**, 952 (1996) [arXiv:hep-ph/9607440]; JETP Lett. **65**, 615 (1997)

- “Radiative energy loss of high energy quarks in finite-size nuclear matter and quark-gluon plasma,” [arXiv:hep-ph/9704255].
- [6] P. B. Arnold, S. Cantrell, W. Xiao, “Stopping distance for high energy jets in weakly-coupled quark-gluon plasmas,” *Phys. Rev.* **D81**, 045017 (2010) [arXiv:0912.3862].
  - [7] H. Liu, K. Rajagopal, U. A. Wiedemann, “Calculating the jet quenching parameter from AdS/CFT,” *Phys. Rev. Lett.* **97**, 182301 (2006) [hep-ph/0605178].
  - [8] S. S. Gubser, D. R. Gulotta, S. S. Pufu and F. D. Rocha, “Gluon energy loss in the gauge-string duality,” *JHEP* **0810**, 052 (2008) [arXiv:0803.1470].
  - [9] Y. Hatta, E. Iancu and A. H. Mueller, “Jet evolution in the  $\mathcal{N}=4$  SYM plasma at strong coupling,” *JHEP* **0805**, 037 (2008) [arXiv:0803.2481].
  - [10] P. M. Chesler, K. Jensen, A. Karch and L. G. Yaffe, “Light quark energy loss in strongly-coupled  $\mathcal{N}=4$  supersymmetric Yang-Mills plasma,” *Phys. Rev. D* **79**, 125015 (2009) [arXiv:0810.1985].
  - [11] D. M. Hofman and J. Maldacena, “Conformal collider physics: Energy and charge correlations,” *JHEP* **0805**, 012 (2008) [arXiv:0803.1467].
  - [12] A. Adare *et al.* [PHENIX Collaboration], “Azimuthal anisotropy of  $\pi^0$  production in Au+Au collisions at  $\sqrt{s_{NN}} = 200$  GeV: Path-length dependence of jet quenching and the role of initial geometry,” *Phys. Rev. Lett.* **105**, 142301 (2010).
  - [13] C. Marquet, T. Renk, “Jet quenching in the strongly-interacting quark-gluon plasma,” *Phys. Lett.* **B685**, 270-276 (2010) [arXiv:0908.0880].
  - [14] J. Jia, R. Wei, “Dissecting the role of initial collision geometry for jet quenching observables in relativistic heavy ion collisions,” *Phys. Rev.* **C82**, 024902 (2010) [arXiv:1005.0645].